Minerals Engineering 50–51 (2013) 77–82

Contents lists available at SciVerse ScienceDirect

Minerals Engineering

journal homepage: www.elsevier.com/locate/mineng

Study of the local critical coalescence concentration (*l-CCC*) of alcohols and salts at bubble formation in two-phase systems

W. Kracht *, H. Rebolledo

Mining Engineering Department, Universidad de Chile, Av. Tupper 2069, Santiago, Chile
Advanced Mining Technology Center, AMTC, Universidad de Chile, Av. Tupper 2007, Santiago, Chile

ARTICLE INFO

Article history:
Received 21 March 2013
Accepted 23 June 2013
Available online 19 July 2013

Keywords:
Froth flotation
Flotation bubbles
Critical coalescence concentration
Flotation reagents

ABSTRACT

The acoustic emissions generated by bubbles when they form are well understood and can be easily measured using a hydrophone and amplifier. Bubbles emit an audible sound not only when they form, but also when two or more coalesce. In this case, however, the amplitude of the sound is higher than after bubble formation. The difference in amplitude is enough to tell between bubble formation and bubble coalescence. Based on this property, the capability of alcohols and salts to prevent coalescence right after bubble formation at a capillary tube was studied. In general, the higher the gas flow rate through the capillary the more intense the collisions between subsequent bubbles, which eventually leads to coalescence, hence a higher reagent concentration in the system is needed to protect the bubbles against it. The reagent concentration at which coalescence is prevented can be seen as a local critical coalescence concentration (*l-CCC*) at the gas flow rate tested. This allows generating a curve of *l-CCC* vs. gas flow rate that can be used for comparison between different reagents. The paper presents results of *l-CCC* curves for alcohols and salts. The *l-CCC* curves show a comparable effect on coalescence prevention between 0.4 M NaCl and 8 ppm MIBC (a common frother), which is in agreement with the literature (Quinn et al., 2007).

1. Introduction

Flotation is widely used to separate particles according to their hydrophobicity. In order to achieve the separation, particles are contacted with bubbles (usually air bubbles) in water. The size and number of bubbles in the flotation cell define the so-called gas dispersion properties, which are known to have a direct impact on flotation performance (Schwarz and Alexander, 2006). For a given gas flow rate, the smaller the bubble size the higher the bubble surface area flux (S_b), and the higher the flotation rate constant (Gorain et al., 1997), hence, small bubbles are preferred in the process.

Frothers are surface-active agents, also called surfactants, widely used in flotation to contribute to the formation of small bubbles (Cho and Laskowski, 2002; Finch et al., 2006, 2008; Grau et al., 2005; Kracht and Finch, 2009a). Analysis of froth formation emphasizes mechanisms that retard coalescence (Pugh, 1996; Harris, 1982), an explanation extended to bubble generation (Kracht and Finch, 2009b). This mechanism has led to the definition of the critical coalescence concentration (*CCC*), which corresponds to the reagent concentration at which bubble coalescence is prevented (Cho and Laskowski, 2002).

Despite the difference between frothers and salts, the latter also reduce bubble size (Machon et al., 1997; Quinn et al., 2007), which, again, is explained by coalescence inhibition (Marrucci and Nicodemo, 1967; Laskowski et al., 2003).

The aim of this project was to study bubble coalescence prevention at bubble formation in a two-phase system (air–water) in the presence of alcohols (surfactants) and salts. Coalescence was detected by analysing the sound that bubbles emit when they form or coalesce.

When a bubble is formed at a capillary, it emits a sound with a characteristic frequency that is related to the size of the bubble being formed (Minnaert, 1933). If the gas flow rate in the capillary is increased, consecutive bubbles start to coalesce at the tip of the capillary. When two bubbles coalesce, they also emit a sound, but of higher amplitude than after bubble formation (Strasberg, 1956; Manasseh et al., 2008). This difference in amplitude can be used to detect bubble coalescence after formation at a capillary tube. Based on this principle, a technique was developed and validated by Kracht and Finch (2009b) to study the effect of reagent type and concentration on coalescence prevention. The same technique is used in this project.

2. Methodology

2.1. Experimental set-up

The experimental set-up (Fig. 1) comprises a 5 L acrylic tank where air bubbles are injected through a glass capillary tube of

* Corresponding author. Fax: +56 2 2978 4985.
E-mail address: wkracht@ing.uchile.cl (W. Kracht).

0892-6875/$ - see front matter © 2013 Elsevier Ltd. All rights reserved.
http://dx.doi.org/10.1016/j.mineng.2013.06.009

254 μm inner diameter (6.4 mm external diameter). The gas used was compressed air, and gas flow rate was measured and controlled with a mass flow meter controller Omega model FMA 5508 (1–100 sccm, standard cubic centimetre per minute). The acoustic emissions are measured with a hydrophone Brüel & Kjaer type 8103 and amplified with a low noise charge amplifier Brüel & Kjaer type 2635. The acoustic emissions were recorded with the freeware audio software Audacity 1.3 beta.

2.2. Reagents

The reagents used comprise alcohols and salts. The alcohols used were the homologous series of *n*-alcohols from propanol to octanol (C_3–C_8) and the isomers: 2 ethyl 1 hexanol; methyl isobutyl carbinol (MIBC); and cyclohexanol. The salts tested were: sodium, potassium, calcium, magnesium, and ferric chloride; copper and zinc sulphate; and sodium carbonate. Table 1 shows a summary of the reagents used.

Solutions were made using Santiago tap water. Between tests, the acrylic tank was emptied and carefully cleaned by rinsing the tank five times with clean (tap) water.

Table 1
Summary of reagents used.

Reagent	Formula	Purity (%)	Supplier
Propanol	$CH_3(CH_2)_2OH$	99.5	Sigma–Aldrich
Butanol	$CH_3(CH_2)_3OH$	⩾99.4	Sigma–Aldrich
Pentanol	$CH_3(CH_2)_4OH$	⩾99	Sigma–Aldrich
Hexanol	$CH_3(CH_2)_5OH$	98	Sigma–Aldrich
Heptanol	$CH_3(CH_2)_6OH$	98	Sigma–Aldrich
Octanol	$CH_3(CH_2)_7OH$	⩾99	Sigma–Aldrich
MIBC	$(CH_3)_2CHCH_2CH(OH)CH_3$	99	Sigma-Aldrich
Cyclohexanol	$C_6H_{11}OH$	99	Sigma–Aldrich
2 Ethyl 1 hexanol	$CH_3(CH_2)_3CH(C_2H_5)CH_2OH$	⩾99.6	Sigma–Aldrich
Sodium chloride	NaCl	>99.5	Merck
Potassium chloride	KCl	>99.5	Merck
Magnesium chloride	$MgCl_2$	99.0	Merck
Calcium chloride	$CaCl_2$	99.0	Merck
Ferric chloride	$FeCl_3$	99.0	Merck
Copper sulphate	$CuSO_4$	99.0	Merck
Zinc sulphate	$ZnSO_4$	99.5	Merck
Sodium carbonate	Na_2CO_3	99.0	Merck

2.3. Technique

The technique is well explained elsewhere (Kracht and Finch, 2009b), and can be summarized as follows: gas (air) is injected through the capillary tube. The bubbling frequency at the capillary increases with the gas flow rate until consecutive bubbles touch each other and eventually coalesce. The coalescence is easily identified from the bubbles acoustic emissions.

For each reagent concentration the gas flow rate at which consecutive bubbles coalesce at the capillary tube is recorded. This allows generating a curve of concentration vs. gas flow rate that represents the maximum gas flow rate that can be injected through the capillary without bubble coalescence at a given reagent concentration. The curve can be seen also as the reagent concentration needed to prevent coalescence at the capillary for a given condition of gas flow rate (i.e., a critical coalescence concentration). The curve represents a boundary that divides coalescence events that occur above the line from the non-coalescence region below it.

2.4. Local critical coalescence concentration (*l*-CCC)

The *CCC*, as defined in the literature (Cho and Laskowski, 2002), is the frother concentration at which bubble coalescence is prevented. This condition is determined from bubble size data as the concentration at which the mean bubble size reaches a minimum. The method based on bubble size data is indirect and does not consider variables that affect the bubble size, other than frother concentration, such as the turbulence and gas flow rate in the cell. On the other hand, the minimum mean bubble size can be reached when bubble break-up events compensate coalescence events, and not necessarily when coalescence is totally prevented, which is not considered by the method either. The acoustic technique, however, represents a direct measurement of the critical coalescence concentration for a given gas flow rate at the capillary, i.e., a local direct measurement of the *CCC*, which will be referred as *l-CCC* in order to differentiate it from the measurement based on bubble size data. Therefore, the curves generated when varying the gas flow rate represent curves of local critical coalescence concentration (*l-CCC*).

2.5. Homologous alcohols

Fig. 2 shows the *l-CCC* curves for the homologous series of alcohols from propanol to octanol (C_3–C_8). For each reagent, the higher

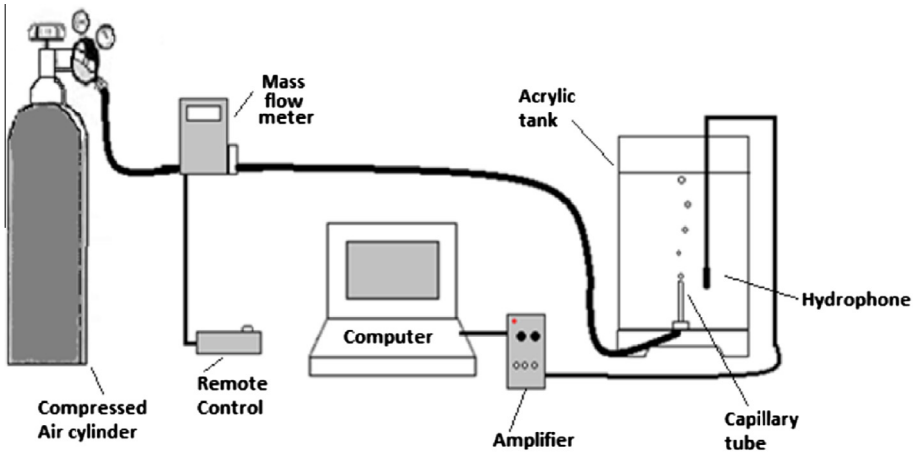

Fig. 1. Experimental set-up for measuring acoustic emissions of bubbles.

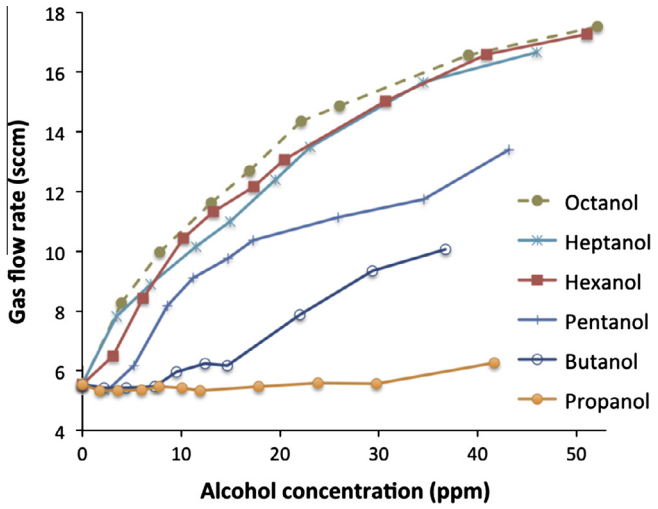

Fig. 2. Curves of coalescence prevention (*l-CCC*) for homologous alcohols.

the curve in the plot the more effective the reagent to prevent coalescence; for instance, at 10 ppm butanol the gas flow rate in the capillary can be increased up to ca. 6 sccm without observing bubble coalescence, whereas at 10 ppm pentanol gas flow rate can be increased up to of ca. 9 sccm without coalescence, which means that 10 ppm pentanol are more effective than 10 ppm butanol to prevent coalescence.

As shown in Fig. 2, coalescence prevention increases with the length of the carbon chain. This is evident from propanol to hexanol (C_3–C_6), and the effect levels out at $C_{>6}$, which is in agreement with the literature (Keitel and Onken, 1982).

The effect that a change in the molecular structure has on coalescence prevention is presented in Fig. 3. Fig. 3 (left) shows the *l-CCC* for three C_6 alcohols. Hexanol and MIBC, a C_6 alcohol with a branched structure, have a similar effect on coalescence prevention. In a prior work, Kracht and Finch (2009b) found that MIBC was more effective than hexanol. The difference may be due to the purity of the reagent used in that work (technical grade). In the current work, both hexanol and MIBC are of high purity (98% and 99% respectively). Cyclohexanol is less effective to prevent coalescence, which is attributed to the cyclic structure of the molecule. Note that, strictly speaking, though it is a C_6 alcohol, this reagent cannot be considered a hexanol isomer since it has two hydrogen atoms less than hexanol and MIBC in its structure.

Fig. 3 (right) shows the *l-CCC* for two C_7 alcohols: heptanol and its isomer 2 ethyl 1 hexanol. In this case a slight difference is observed, the branched structured C_7 alcohol being more effective than the normal heptanol to prevent coalescence.

2.6. Effect of salts on coalescence prevention

Fig. 4 shows the *l-CCC* curves for salts. As it can be seen from the figure, some of the salts present a behaviour that differs from that of alcohols. In the case of alcohols a well-defined *l-CCC* curve was observed. Some of the salts, however, did not show a sharp transition between non-coalescence and coalescence, but a transition zone where sporadic coalescence (or partial coalescence prevention) was observed. In other words, there is not a well-defined boundary between non-coalescence and coalescence region, which means that when the gas flow rate is increased, it reaches a point (Q_1) where only some of the coalescence events are prevented in a process that appears to be random. If the gas flow rate is further increased, it eventually reaches a point (Q_2) where coalescence between consecutive bubbles is not prevented at all. Since below Q_1 there are no coalescence events, and between Q_1 and Q_2 there is partial coalescence prevention (sporadic coalescence events), these gas flow rates allow defining the transition zone, which corresponds to that between the complete coalescence prevention (Q_1) and the partial coalescence prevention (Q_2) in Fig. 4.

A transition zone between non-coalescence and coalescence was observed for sodium, potassium, and calcium chloride. It was less evident for magnesium chloride, and almost negligible for the rest of the salts tested. These salts, namely copper and zinc sulphate, ferric chloride, and sodium carbonate, show the same behaviour as alcohols.

The transition zone has been previously reported in the literature. Christenson et al. (2008) for instance, measured the fraction of contacting bubble pairs that coalesce as a function of electrolyte concentration. They found that both, NaCl and $CaCl_2$ show a somehow smooth transition to bubble coalescence inhibition. The same was observed by Nguyen et al. (2012) for NaCl in a small bubble column.

Kurniawan et al. (2011) showed that $MgCl_2$ reduced bubble coalescence more than NaCl in the froth phase of a laboratory flotation cell. This is in agreement with the results of coalescence prevention presented in Fig. 4 for both salts. The curve of coalescence prevention for magnesium chloride is above that of sodium chloride. This, together with the fact that sodium chloride exhibits a more pronounced transition zone than magnesium chloride, means the latter is more effective than NaCl to prevent bubble coalescence.

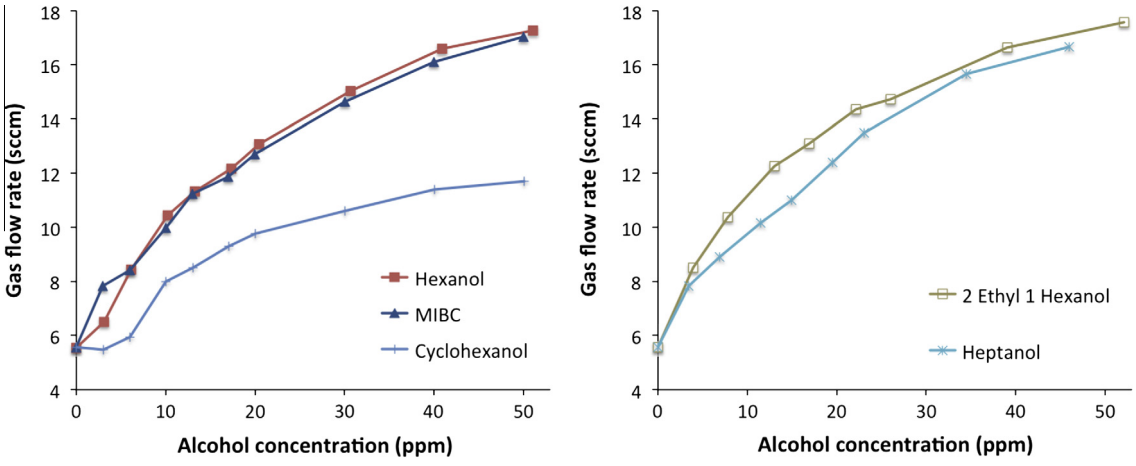

Fig. 3. Effect of reagent structure (alcohol) on coalescence prevention.

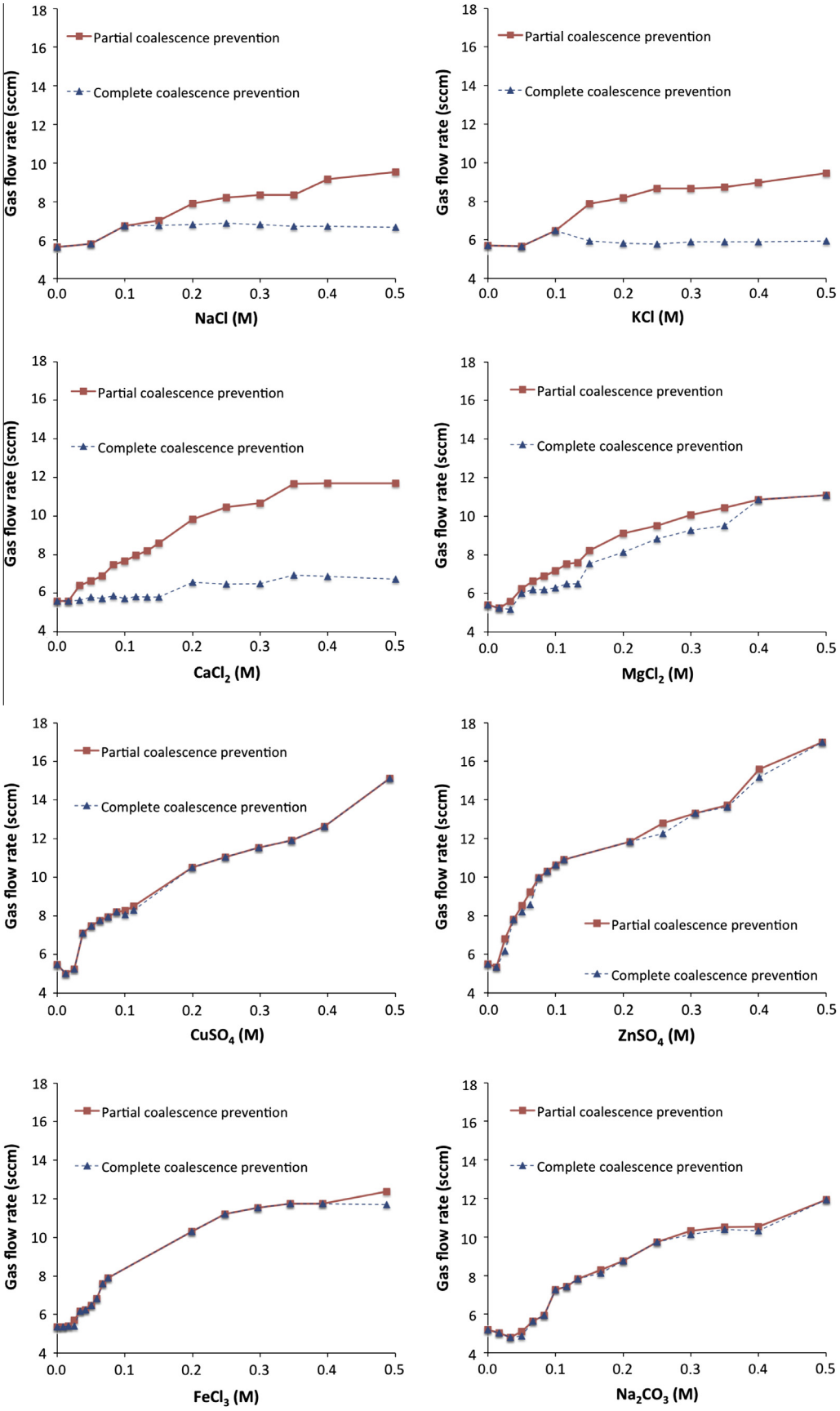

Fig. 4. Curves of coalescence prevention (*l-CCC*) for salts.

According to Weissenborn and Pugh (1996), the surface tension gradients generated in presence of electrolytes are significantly smaller than those generated by surfactants, therefore, the coalescence prevention cannot be attributed to Gibbs elasticity as in the case of frothers. Safouane and Langevin (2009), on the other hand, show that there is no significant viscoelasticity below 2 M NaCl or $CaCl_2$, a concentration that is above the concentrations tested in the current work. It has been proposed that electrolyte has an effect on the small-scale structure of solution at the interface that may determine coalescence inhibition (Henry et al., 2007). This effect may be related to the affinity of salt ions to water molecules (Nguyen et al., 2012), an explanation that focuses on the behaviour of ions at the interface. When cations and anions have different degrees of affinity for the approach to the interface, this results in a repulsive interaction between bubble surfaces due to the electrical double layer (Marcelja, 2006), and coalescence is inhibited.

2.7. Combined effect of MIBC and NaCl

Seawater has a high concentration of NaCl (around 0.5–0.6 M), with important secondary ions such as, sulphate ions, magnesium ions and bicarbonate ions (Castro, 2012). On the other hand, several concentrators are either using or considering the use of seawater to satisfy the water demand of the process; therefore, the effect that high concentrations of sodium chloride (NaCl) has on the process, in this case on coalescence prevention, is of great interest.

Fig. 5 shows the combined effect of the common frother MIBC and a high concentration of NaCl (0.5 M). The presence of 0.5 M NaCl in the solution displaces the *l-CCC* curve of MIBC upwards, increasing its ability to prevent coalescence. Despite the fact that sodium chloride alone shows two regions, namely total coalescence prevention and partial coalescence prevention, the combined effect of MIBC and NaCl 0.5 M does not show sporadic coalescence events, but a well defined *l-CCC* curve. From a practical point of view, this observation suggests that concentrators operating with seawater would need a lower frother concentration to prevent bubble coalescence.

2.8. Equivalent frother (MIBC) concentration

Since both alcohols and salts have the capability to prevent bubble coalescence, it is interesting to establish an equivalent concentration between them based on a comparison of their *l-CCC* curves. Fig. 6 shows the determination of the equivalent concentration between MIBC, an alcohol and also a common frother (upper axis) and NaCl (lower axis). The figure shows that a concentration of 0.4 M NaCl is comparable to 8 ppm MIBC, which is in agreement with the equivalent concentration determined using gas holdup in the collection zone as a way of comparison for a three-phase system (Quinn et al., 2007). From Fig. 5 it can be seen that 0.5 M NaCl is equivalent to ca. 9.5 ppm MIBC (auxiliary lines for determination not shown). This equivalence has been found (Bournival et al., 2012) to be related to the comparable coalescence times between relatively concentrated solutions of NaCl and small amounts of MIBC.

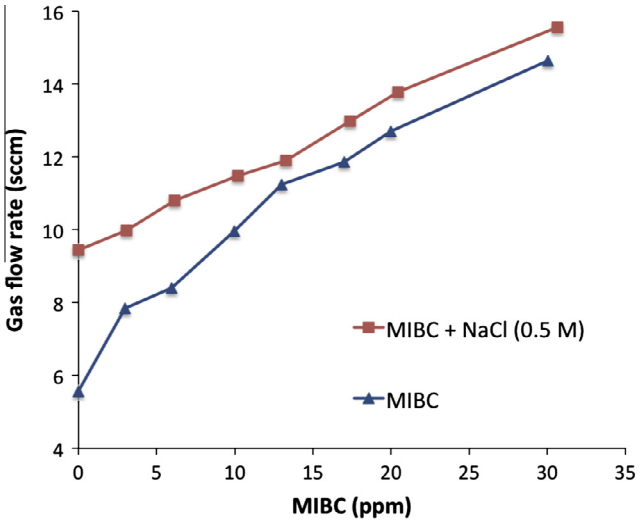

Fig. 5. Effect of salt (NaCl, 0.5 M) on the *l-CCC* curve of MIBC.

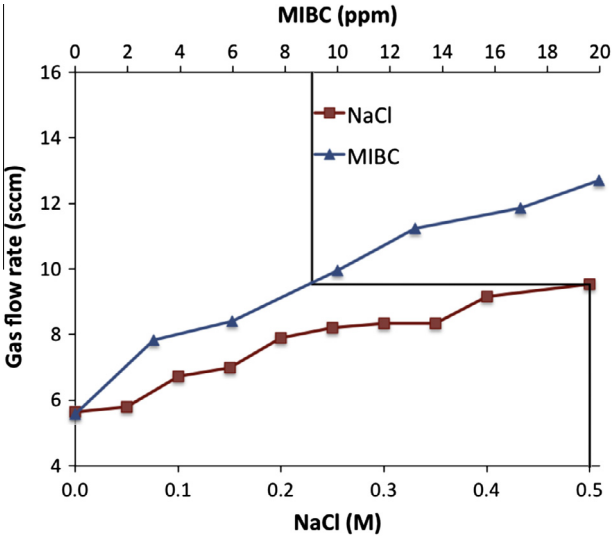

Fig. 6. Determining equivalent frother (MIBC) concentration.

3. Conclusions

The concept of local critical coalescence concentration (*l-CCC*) curve is introduced. The *l-CCC* represents a direct measurement of the critical coalescence concentration at a given gas flow rate. The *l-CCC* curves can be used to compare reagents in terms of their ability to prevent bubble coalescence.

The ability of the homologous series of alcohols (C_3–C_8) to prevent coalescence increases with the number of carbons up to C_6 (hexanol). After that (C_7–C_8) the ability levels out. The effect of molecular structure is also presented. It is observed that there is a great difference between an aliphatic linear (hexanol) or branched (MIBC) and the cyclic C_6 alcohol (cyclohexanol). In the case of linear vs. branched structures (C_6, C_8) the difference in coalescence prevention is minor. For all the alcohols tested, a well-defined *l-CCC* curve was observed.

Salts also show coalescence prevention, however, unlike alcohols, some of the salts tested did not show a sharp transition between non-coalescence and coalescence, but a transition zone where sporadic coalescence was observed. A transition zone between non-coalescence and coalescence was observed for sodium, potassium, and calcium chloride. The transition zone was less evident for magnesium chloride, and almost negligible for the rest of the salts tested. In that sense, copper and zinc sulphate, ferric chloride, and sodium carbonate, presented the same behaviour than alcohols.

It was found that the *l-CCC* curve for MIBC in the presence of 0.5 M NaCl (concentration typical of seawater) was displaced upwards compared to the *l-CCC* curve for MIBC in fresh water (with no salt). From a practical point of view, this observation suggests

that concentrators operating with seawater would need a lower frother concentration to prevent bubble coalescence.

Finally, the *l-CCC* curves were used to establish an equivalent concentration between the alcohol and also common frother (MIBC) and sodium chloride. The *l-CCC* curves show a comparable effect on coalescence prevention between 0.4 M NaCl and 8 ppm MIBC, which is in agreement with the literature.

Acknowledgements

The authors would like to acknowledge the Chilean National Commission for Scientific and Technological Research (CONICYT) for funding this research through the National Fund for Scientific and Technological Development (FONDECYT), project number 1110173.

References

Bournival, G., Pugh, R.J., Ata, S., 2012. Examination of NaCl and MIBC as bubble coalescence inhibitor in relation to froth flotation. Minerals Engineering 25, 47–53.

Castro, S., 2012. Challenges in flotation of Cu–Mo sulfide ores in sea water. Water in Mineral Processing. In: Proceedings of the First International Symposium. SME. pp. 29–40.

Cho, Y.S., Laskowski, J.S., 2002. Effect of flotation frothers on bubble size and foam stability. International Journal of Mineral Processing 64, 69–80.

Christenson, H.K., Bowen, R.E., Carlton, J.A., Denne, J.R.M., Lu, Y., 2008. Electrolytes that show a transition to bubble coalescence at high concentrations. Journal of Physical Chemistry C 112, 794–796.

Finch, J.A., Nesset, J.E., Acuna, C., 2008. Role of frother in bubble production and behaviour in flotation. Minerals Engineering 21, 949–957.

Finch, J.A., Gélinas, S., Moyo, P., 2006. Frother-related research at McGill University. Minerals Engineering 19, 726–733.

Gorain, B.K., Franzidis, J.P., Manlapig, E.V., 1997. Studies on impeller type, impeller speed and air flow rate in an industrial flotation cell – part 4: effect of bubble surface area flux on flotation performance. Minerals Engineering 10, 367–379.

Grau, R.A., Laskowski, J.S., Heiskanen, K., 2005. Effect of frothers on bubble size. International Journal of Mineral Processing 76, 225–233.

Harris, P.J., 1982. In: King, R.P. (Ed.), Principles of Flotation. Chapter 13: Frothing phenomena and frothers. South African Institute of Mining and Metallurgy Monograph Series No.3.

Henry, C.L., Casuarina, N.D., Scruton, L., Craig, V.S.J., 2007. Ion-specific coalescence of bubbles in mixed electrolyte solutions. Journal of Physical Chemistry C 111, 1015–1023.

Keitel, G., Onken, U., 1982. Inhibition of bubble coalescence by solutes in air/water dispersions. Chemical Engineering Science 37, 1635–1638.

Kracht, W., Finch, J.A., 2009a. Bubble break-up and the role of frother and salt. International Journal of Mineral Processing 92, 153–161.

Kracht, W., Finch, J.A., 2009b. Using sound to study bubble coalescence. Journal of Colloid and Interface Science 332, 237–245.

Kurniawan, A.U., Ozdemir, O., Nguyen, A.V., Ofori, P., Firth, B., 2011. Flotation of coal particles in $MgCl_2$, NaCl, and $NaClO_3$ solutions in the absence and presence of Dowfroth 250. International Journal of Mineral Processing 98, 137–144.

Laskowski, J.S., Cho, Y.S., Ding, K., 2003. Effect of frothers on bubble size and foam stability in potash ore flotation systems. Canadian Journal of Chemical Engineering 81, 63–69.

Machon, V., Pacek, A.W., Nienow, A.W., 1997. Bubble sizes in electrolyte and alcohol solutions in a turbulent stirred vessel. Transaction I Chemistry E 75 (A), 339–348.

Marcelja, S., 2006. Selective coalescence of bubbles in simple electrolytes. Journal of Physical Chemistry B 110, 13062–13067.

Marrucci, G., Nicodemo, L., 1967. Coalescence of gas bubbles in aqueous solutions of inorganic electrolytes. Chemical Engineering Science 22, 1257–1265.

Manasseh, R., Riboux, G., Risso, F., 2008. Sound generation on bubble coalescence following detachment. International Journal of Multiphase Flow 34, 938–949.

Minnaert, M., 1933. On musical air bubbles and the sound of running water. Philosophical Magazine 16, 235–248.

Nguyen, P.T., Hampton, M.A., Nguyen, A.V., Birkett, G.R., 2012. The influence of gas velocity, salt type and concentration on transition concentration for bubble coalescence inhibition and gas holdup. Chemical Engineering Research and Design 90, 33–39.

Pugh, R.J., 1996. Foaming, foam films, antifoaming and defoaming. Advances in Colloid and Interface Science 64, 67–102.

Quinn, J.J., Kracht, W., Gomez, C.O., Gagnon, C., Finch, F.A., 2007. Comparing the effect of salts and frother (MIBC) on gas dispersion and froth properties. Minerals Engineering 20, 1296–1302.

Safouane, M., Langevin, D., 2009. Surface viscoelasticity of concentrated salt solutions: specific ion effects. ChemPhysChem 10, 222–225.

Schwarz, S., Alexander, D., 2006. Gas dispersion measurements in industrial cells. Minerals Engineering 19, 554–560.

Strasberg, M., 1956. Gas bubbles as sources of sound in liquid. Journal of the Acoustical Society of America 28, 20–26.

Weissenborn, P.K., Pugh, R.J., 1996. Surface tension of aqueous solutions of electrolytes: relationship with ion hydration, oxygen solubility, and bubble coalescence. Journal of Colloid and Interface Science 184, 341–346.